

# Alkali-metal complexes of a pendant-arm tetraaza macrocycle. Equilibrium, inter- and intra-molecular exchange processes

Sonya L. Whitbread,<sup>a</sup> Steve Politis,<sup>a</sup> Ashley K. W. Stephens,<sup>a</sup> Jeremy B. Lucas,<sup>a</sup> Ramesh Dhillon,<sup>a</sup> Stephen F. Lincoln<sup>\*a</sup> and Kevin P. Wainwright<sup>b</sup>

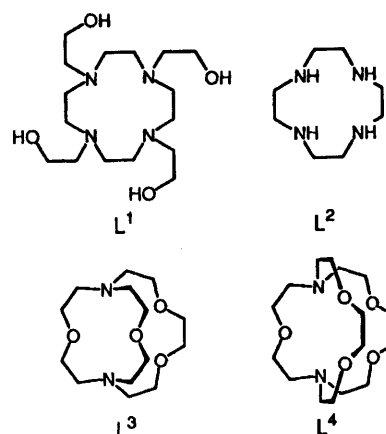
<sup>a</sup> Department of Chemistry, University of Adelaide, Adelaide, SA 5005, Australia

<sup>b</sup> School of Physical Sciences, The Flinders University of South Australia, GPO Box 2100, Adelaide, SA 5001, Australia

The stabilities  $\log(K/\text{dm}^3 \text{ mol}^{-1})$  of  $[\text{ML}^1]^+$  formed by 1,4,7,10-tetrakis(2-hydroxyethyl)-1,4,7,10-tetraazacyclododecane ( $\text{L}^1$ ) were found to vary with  $\text{M}^+$  in the sequence  $\text{Li}^+$  ( $8.07 \pm 0.05$  and  $8.90 \pm 0.05$ ),  $\text{Na}^+$  ( $6.66 \pm 0.05$  and  $7.49 \pm 0.05$ ),  $\text{K}^+$  ( $3.40 \pm 0.05$  and  $5.91 \pm 0.05$ ),  $\text{Rb}^+$  ( $3.00 \pm 0.05$  and  $4.23 \pm 0.05$ ),  $\text{Cs}^+$  ( $2.90 \pm 0.05$  and  $4.04 \pm 0.05$ ) and  $\text{Ag}^+$  ( $9.35 \pm 0.04$  and  $14.00 \pm 0.05$ ), in acetonitrile and propylene carbonate, respectively, determined by potentiometric titration at 298.2 K and  $I = 0.05 \text{ mol dm}^{-3}$  ( $\text{NET}_4\text{ClO}_4$ ). Complexes of the parent macrocycle 1,4,7,10-tetraazacyclododecane ( $\text{L}^2$ ) are less stable. For the monomolecular decomplexation of  $[\text{NaL}^1]^+$  in acetonitrile and propylene carbonate the values  $k_d$  (298.2 K) =  $78.5 \pm 1.0$  and  $26.1 \pm 0.6 \text{ s}^{-1}$ ,  $\Delta H_d^\ddagger = 49.2 \pm 0.3$  and  $57.7 \pm 0.4 \text{ kJ mol}^{-1}$ , and  $\Delta S_d^\ddagger = -43.7 \pm 0.9$  and  $-24.0 \pm 1.0 \text{ J K}^{-1} \text{ mol}^{-1}$ , respectively, were determined by  $^{23}\text{Na}$  NMR spectroscopy. Carbon-13 NMR spectroscopy showed that for the enantiomerisation of square-antiprismatic  $[\text{LiL}^1]^+$ ,  $[\text{NaL}^1]^+$  and  $[\text{KL}^1]^+$  in methanol,  $k_e$  (298.2 K) =  $18\,300 \pm 3100$ ,  $7100 \pm 220$  and  $7010 \pm 200 \text{ s}^{-1}$ ,  $\Delta H_e^\ddagger = 41.3 \pm 1.3$ ,  $24.6 \pm 0.5$  and  $53.7 \pm 0.6 \text{ kJ mol}^{-1}$ , and  $\Delta S_e^\ddagger = -24.8 \pm 5.9$ ,  $-88.6 \pm 1.8$  and  $8.8 \pm 2.3 \text{ J K}^{-1} \text{ mol}^{-1}$ , respectively. For  $[\text{LiL}^1]^+$  and  $[\text{NaL}^1]^+$  enantiomerisation occurs much more rapidly than intermolecular exchange of  $\text{L}^1$ , but for  $[\text{KL}^1]^+$  enantiomerisation occurs predominantly through intermolecular exchange of  $\text{L}^1$ .

Since the characterisation of the alkali-metal complexes formed by ionophoric antibiotics, coronands and cryptands, the factors affecting the stability and substitution lability of such complexes in solution have elicited considerable interest which has resulted in the synthesis of a wide range of alkali-metal complexing agents.<sup>1-7</sup> Among these is 1,4,7,10-tetrakis(2-hydroxyethyl)-1,4,7,10-tetraazacyclododecane ( $\text{L}^1$ ) which was the first pendant-arm tetraaza macrocycle whose alkali-metal complexes were the subject of quantitative equilibrium and kinetic studies of inter- and intra-molecular exchange processes.<sup>6,7</sup> The variation of the stability of  $[\text{ML}^1]^+$  with  $\text{M}^+$  in the sequence  $\text{Li}^+ < \text{Na}^+ > \text{K}^+ > \text{Rb}^+ > \text{Cs}^+$  in methanol and dimethylformamide was attributed to a changing balance between the solvation energies of  $\text{M}^+$  and the ability of  $\text{L}^1$  to adopt optimum conformations for co-ordination as the ionic radii<sup>8</sup> of  $\text{M}^+$  changed. In this study the stability and lability of  $[\text{ML}^1]^+$  in the weaker donor solvents acetonitrile and propylene carbonate (4-methyl-1,3-dioxolan-2-one) are determined to provide a broader understanding of the effect of solvation changes on these characteristics, and an indication of the effects of the pendant arms of  $\text{L}^1$  on complexation is sought through a comparison with the analogous complexes of the parent macrocycle 1,4,7,10-tetraazacyclododecane ( $\text{L}^2$ ).

In the solid state  $\text{L}^1$  acts as a penta-, hepta- and octadentate ligand in  $[\text{LiL}^1]^+$ ,  $[\text{NaL}^1]^+$  and  $[\text{KL}^1]^+$ , respectively, in which one, three and four of the 2-hydroxyethyl pendant arms are co-ordinated.<sup>9-11</sup> Such differences in co-ordination in solution would be expected significantly to influence the stability and lability of  $[\text{ML}^1]^+$ . However, a preliminary solution study showed  $\text{L}^1$  to be octadentate in  $[\text{NaL}^1]^+$  which formed  $\Delta$  and  $\Lambda$  enantiomers,<sup>7</sup> and this study seeks fully to establish the denticity of  $\text{L}^1$  in  $[\text{ML}^1]^+$  in solution and the mechanistic relationship between enantiomerisation and intermolecular  $\text{M}^+$  and  $\text{L}^1$  exchange on  $[\text{ML}^1]^+$ .



## Experimental

The preparations<sup>12,13</sup> of  $\text{L}^1$  and  $\text{L}^2$  and the sources of the alkali-metal and silver perchlorates were similar to those described in the literature.<sup>6</sup> The salt  $\text{NET}_4\text{ClO}_4$  was prepared by precipitation from aqueous  $\text{NET}_4\text{Br}$  (BDH) solution with an excess of  $\text{HClO}_4$  and was recrystallised from water until no acid or bromide was detectable. Stoichiometric amounts of  $\text{K}_2\text{CO}_3$  (BDH) and  $\text{CF}_3\text{SO}_3\text{H}$  (Fluka) were mixed in water to prepare  $\text{K}(\text{O}_3\text{SCF}_3)$  which was twice recrystallised. All of the salts were vacuum dried at 353–363 K for 48 h, and then stored over  $\text{P}_2\text{O}_5$  under vacuum. **CAUTION:** anhydrous perchlorate salts are potentially powerful oxidants and should be handled with care.

Acetonitrile and propylene carbonate were purified and dried by literature methods,<sup>14</sup> and stored under nitrogen over Linde 3 Å molecular sieves. Their water content was below the Karl-Fischer detection level of approximately 50 ppm. Carbon-12-

**Table 1** Variation of stability of  $[\text{ML}^n]^+$  with  $\text{M}^+$  and solvent at 298.2 K and  $I = 0.05 \text{ mol dm}^{-3}$  ( $\text{NEt}_4\text{ClO}_4$ )

Complex	Solvent	$D_N$	$\log(K/\text{dm}^3 \text{ mol}^{-1})^a$					
			$\text{M}^+ = \text{Li}^+$	$\text{Na}^+$	$\text{K}^+$	$\text{Rb}^+$	$\text{Cs}^+$	$\text{Ag}^+$
$[\text{ML}^1]^+$	Acetonitrile <sup>b</sup>	14.1 <sup>c</sup>	$8.07 \pm 0.05$	$6.66 \pm 0.05$	$3.40 \pm 0.05$	$3.00 \pm 0.05$	$2.90 \pm 0.05$	$9.35 \pm 0.05$
	Propylene carbonate <sup>b</sup>	15.1 <sup>c</sup>	$8.90 \pm 0.05$	$7.49 \pm 0.05$	$5.91 \pm 0.05$	$4.23 \pm 0.05$	$4.04 \pm 0.05$	$14.00 \pm 0.05$
	Methanol <sup>d</sup>	23.5 <sup>c</sup>	3.09	4.53	2.43	2.20	1.90	12.57
	Dimethylformamide <sup>d</sup>	26.6 <sup>c</sup>	2.99	3.37	1.59	1.39	1.23	11.16
$[\text{ML}^2]^+$	Acetonitrile <sup>b</sup>	14.1	$6.90 \pm 0.05$	$3.60 \pm 0.05$	$2.90 \pm 0.05$	$2.82 \pm 0.05$	$2.78 \pm 0.05$	$9.43 \pm 0.05$
	Propylene carbonate <sup>b</sup>	15.1	$5.6 \pm 0.1$	$5.5 \pm 0.1$	$4.8 \pm 0.1$	$4.1 \pm 0.1$	<i>f</i>	$11.3 \pm 0.1$
	Dimethylformamide <sup>b</sup>	26.6	$2.1 \pm 0.5$	<2	<2	<2	<2	$9.1 \pm 0.5$
$[\text{ML}^3]^+$	Methanol <sup>g</sup>	23.3	8.04	6.1	2.3	1.9		10.60
$[\text{ML}^4]^+$	Methanol <sup>g</sup>	23.3	5.38	9.65	8.54	6.74	4.33	14.64

<sup>a</sup> Errors represent one standard deviation. <sup>b</sup> This work. <sup>c</sup> Ref. 17. <sup>d</sup> Ref. 6. <sup>e</sup> Ref. 18. <sup>f</sup> Low solubility. <sup>g</sup> Ref. 16.

enriched  $[\text{}^2\text{H}_4]$ methanol (Aldrich) was used as received. Solutions of anhydrous metal perchlorates [or  $\text{K}(\text{O}_3\text{SCF}_3)$  for  $^{13}\text{C}$  NMR studies, as  $\text{KClO}_4$  was insufficiently soluble to give reasonable resonance intensities] and  $\text{L}^1$  and  $\text{L}^2$  were prepared under dry nitrogen in a glove-box. For  $^{13}\text{C}$  NMR studies, methanol solutions of the appropriate alkali-metal salt and  $\text{L}^1$  were transferred to tightly stoppered 5 mm NMR tubes. For  $^{23}\text{Na}$  NMR studies, solutions were degassed and sealed under vacuum in 5 mm NMR tubes which were coaxially mounted in 10 mm NMR tubes containing either  $\text{D}_2\text{O}$  or  $[\text{}^2\text{H}_6]$ acetone which provided the  $^2\text{H}$  lock signal.

The  $^{13}\text{C}$  and  $^{23}\text{Na}$  NMR spectra were run at 75.47 and 79.39 MHz, respectively, on a Bruker CXP-300 spectrometer. In the  $^{13}\text{C}$  experiment 6000 transients were accumulated in an 8192 data-point base over a 3000 Hz spectral width for each solution prior to Fourier transformation. In the  $^{23}\text{Na}$  experiments 1000–6000 transients were accumulated in a 2048 data-point base over an 8000 Hz spectral width for each solution. The solution temperature was controlled to within  $\pm 0.3$  K using a Bruker B-VT 1000 temperature controller. The Fourier-transformed spectra were subjected to complete lineshape analyses<sup>15</sup> on a VAX 11-780 computer to obtain kinetic data. The temperature-dependent  $^{13}\text{C}$  and  $^{23}\text{Na}$  linewidths and chemical shifts employed in the lineshape analysis were obtained from extrapolation from low temperatures where no exchange-induced modification occurred. Stability constants,  $K$  ( $=[\text{ML}^1]^+ / [\text{M}^+][\text{L}^1]$ ), were determined by triplicate potentiometric titrations using equipment and methods similar to those described in the literature.<sup>6,16</sup>

## Results and Discussion

### Equilibrium studies

In acetonitrile and propylene carbonate  $K$  varies in magnitude with  $\text{M}^+$  in the sequence  $\text{Li}^+ > \text{Na}^+ > \text{K}^+ > \text{Rb}^+ > \text{Cs}^+$ , whereas in methanol and dimethylformamide the sequence is  $\text{Li}^+ < \text{Na}^+ > \text{K}^+ > \text{Rb}^+ > \text{Cs}^+$  (Table 1). These variations with change in the electron-donating power of the solvent, as reflected by the Gutmann donor number ( $D_N$ ),<sup>17,18</sup> are consistent with (i) the solvation energy of the alkali-metal ion, (ii) the electron-donating power of the donor atoms of  $\text{L}^1$  and (iii) the ability of  $\text{L}^1$  to assume a conformation which optimises bonding with  $\text{M}^+$  dominating the stability of  $[\text{ML}^1]^+$ . Thus, as  $\text{M}^+$  becomes more strongly solvated with increase in  $D_N$  the balance among (i)–(iii) changes and the order of  $[\text{ML}^1]^+$  stability changes with the solvent, and stability decreases for a particular  $[\text{ML}^1]^+$ . (The latter trend is also seen for  $[\text{AgL}^1]^+$ , however, the stability of  $[\text{AgL}^1]^+$  is substantially greater than that of its alkali-metal analogues because of the strong affinity of the soft acid<sup>19,20</sup>  $\text{Ag}^+$  for the four nitrogens of the tetraazamacrocyclic ring.<sup>21,22</sup> In accord with this the nitrogen-donor acetonitrile competes more effectively for  $\text{Ag}^+$  than do

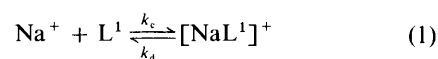
the three oxygen-donor solvents and the stability of  $[\text{AgL}^1]^+$  decreases.)

Our  $^{13}\text{C}$  NMR studies in  $^{12}\text{C}$ -enriched  $[\text{}^2\text{H}_4]$ methanol show all four pendant arms to be bound in  $[\text{LiL}^1]^+$ ,  $[\text{NaL}^1]^+$  and  $[\text{KL}^1]^+$  as is discussed below (and it is assumed that a similar situation prevails with  $[\text{RbL}^1]^+$  and  $[\text{CsL}^1]^+$  which were not amenable to  $^{13}\text{C}$  NMR studies due to the low solubilities of  $\text{Rb}^+$  and  $\text{Cs}^+$  salts). As acetonitrile and propylene carbonate compete less effectively with  $\text{L}^1$  for  $\text{M}^+$  than does methanol, it is probable that  $[\text{ML}^1]^+$  is similarly coordinated in these solvents also, and that the variation in  $[\text{ML}^1]^+$  stability does not arise from coordination variations. The alkali-metal complexes of the parent ligand,  $\text{L}^2$ , are less stable than those of  $\text{L}^1$ , consistent with the additional binding of  $\text{M}^+$  by pendant arms stabilising  $[\text{ML}^1]^+$  (Table 1).

The solvent dependence of the variation of  $[\text{ML}^1]^+$  stability with  $\text{M}^+$  contrasts with the independence of solvent on the stability variations of  $[\text{ML}^3]^+$  and  $[\text{ML}^4]^+$  formed by the cryptands 4,7,13,18-tetraoxa-1,10-diazabicyclo[8.5.5]icosane ( $\text{L}^3$ ) and 4,7,13,16,21-pentaoxa-1,10-diazabicyclo[8.8.5]tricosane ( $\text{L}^4$ ) which selectively complex  $\text{Li}^+$  and  $\text{Na}^+$ , respectively, in acetonitrile, propylene carbonate, methanol and dimethylformamide.<sup>16,23</sup> This, and the higher stabilities of  $[\text{ML}^3]^+$  and  $[\text{ML}^4]^+$  in these solvents (as shown for methanol in Table 1) are consistent with  $\text{L}^1$  more readily adapting to the size of  $\text{M}^+$  than is the case for relatively rigid  $\text{L}^3$  and  $\text{L}^4$  which have preformed cavities of approximate radii 80 and 110 pm,<sup>4,5</sup> respectively, which are close to the six-coordinate radius of  $\text{Li}^+$  (76 pm) and the seven-coordinate radius of  $\text{Na}^+$  (112 pm).<sup>8</sup>

### $^{23}\text{Na}$ NMR intermolecular exchange studies

The temperature-dependent coalescences of the  $^{23}\text{Na}$  resonances arising from the exchange of  $\text{Na}^+$  between the  $[\text{NaL}^1]^+$  and solvated environments in acetonitrile and propylene carbonate (Fig. 1) yield the mean lifetime of  $\text{Na}^+$  in  $[\text{NaL}^1]^+$ ,  $\tau_c$ , through complete lineshape analyses.<sup>15</sup> For a particular solution  $\tau_c/X_c = \tau_s/X_s$ , where  $\tau_s$  is the mean lifetime of  $\text{Na}^+$  in the solvated environment and  $X_c$  and  $X_s$  are the corresponding mole fractions. For a given solvent, the magnitudes and temperature variations of  $\tau_c$  for the solutions studied are very similar (Fig. 2) consistent with  $\tau_c$  for  $[\text{NaL}^1]^+$  being independent of  $[\text{Na}^+(\text{solv})]$  and the absence of  $\text{Na}^+(\text{solv})$  from the rate-determining step of the dominant pathway for exchange of  $\text{Na}^+$  on  $[\text{NaL}^1]^+$ . Thus, a monomolecular mechanism operates for the decomplexation of  $\text{Na}^+$  from  $[\text{NaL}^1]^+$  as shown in equation (1) where  $k_d$  ( $= 1/\tau_c$ ) and



$k_c$  ( $= k_d K$ ) are the decomplexation and complexation rate constants, respectively. This is also the case in methanol and

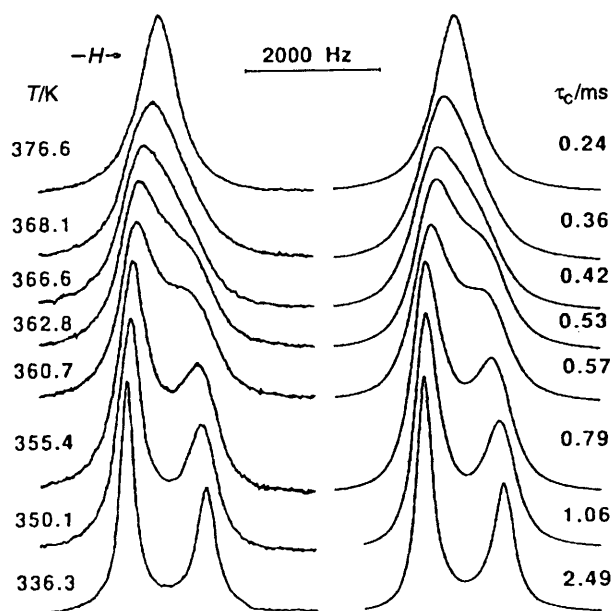


**Fig. 1** Typical exchange-modified 79.39 MHz  $^{23}\text{Na}$  NMR spectra of a propylene carbonate solution of solvated  $\text{Na}^+$  ( $0.0635 \text{ mol dm}^{-3}$ ) and  $[\text{NaL}^1]^+$  ( $0.0365 \text{ mol dm}^{-3}$ ). Experimental temperatures and spectra appear to the left of the figure, and the best-fit calculated lineshapes and corresponding  $\tau_c$  values to the right

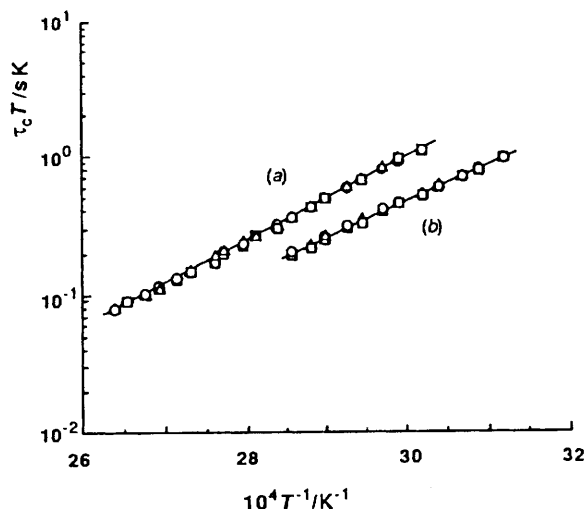


**Fig. 2** Temperature variation of  $\tau_c$  for  $[\text{NaL}^1]^+$ : (a) propylene carbonate solutions (i)–(iii) which were  $0.0674$ ,  $0.0560$  and  $0.0365 \text{ mol dm}^{-3}$  in  $[\text{NaL}^1]^+$  and  $0.0326$ ,  $0.0440$  and  $0.0635 \text{ mol dm}^{-3}$  in  $\text{Na}^+$  (solv), and are represented by circles, squares and triangles, respectively; (b) acetonitrile solutions (iv)–(vi) which were  $0.0747$ ,  $0.0561$  and  $0.0398 \text{ mol dm}^{-3}$  in  $[\text{NaL}^1]^+$  and  $0.0266$ ,  $0.0452$  and  $0.0615 \text{ mol dm}^{-3}$  in  $\text{Na}^+$  (solv), and are represented by circles, squares and triangles, respectively. The solid lines represent the linear regression fits of the combined sets of data obtained in each solvent to equation (2)

dimethylformamide.<sup>6</sup> The parameters for the decomplexation of  $[\text{NaL}^1]^+$  (Table 2) are derived from the temperature variation of  $\tau_c$  through equation (2).

$$k_d = 1/\tau_c = (k_B T/h) \exp[-(\Delta H_d^\ddagger/RT) + (\Delta S_d^\ddagger/R)] \quad (2)$$

The formation of an encounter-complex, in which the first solvation shell of  $\text{Na}^+$  is in contact with  $\text{L}^1$ , is probably the fastest step in the process leading to the formation of  $[\text{NaL}^1]^+$  such that the second-order rate constant  $k_c$  is the product of the encounter-complex stability constant and the rate constant for the slowest monomolecular complexation step. The slowest monomolecular decomplexation step is characterized by  $k_d$ . These slowest steps in the multistep complexation and

decomplexation processes cannot be identified from the available data. For the three oxygen-donor solvents,  $k_c$  and  $k_d$  increase and decrease, respectively, as donor strength decreases consistent with desolvation and resolution of  $\text{Na}^+$  substantially controlling the relative magnitudes of  $k_c$  and  $k_d$ , respectively, and thereby the relative order of stability. The deviation of the data in acetonitrile from this broad trend may be a consequence of the change to a nitrogen-donor atom. In propylene carbonate, methanol and dimethyl formamide,  $k_d$  for  $[\text{NaL}^3]^+$  and  $[\text{NaL}^4]^+$  are much smaller than that for  $[\text{NaL}^1]^+$  as is seen for methanol in Table 2.<sup>16,24,25</sup> This is consistent with the lesser flexibility of the cryptands hindering decomplexation, which is particularly marked for  $\text{L}^4$  which has a cavity of optimum size to accommodate  $\text{Na}^+$ ,<sup>4,5</sup> and is reflected in  $k_c$  for  $[\text{NaL}^4]^+$  being substantially greater than that for  $[\text{NaL}^3]^+$  and also for  $[\text{NaL}^1]^+$ .

### Carbon-13 intra- and inter-molecular exchange studies

Under slow-exchange conditions at 219.3 K in  $^{12}\text{C}$ -enriched  $[\text{H}_4]$ methanol the  $^{13}\text{C}$ - $\{^1\text{H}\}$  NMR spectra of  $[\text{ML}^1]^+$  consist of four resonances. Thus, for  $[\text{LiL}^1]^+$ ,  $[\text{NaL}^1]^+$  and  $[\text{KL}^1]^+$ , respectively,  $\delta$  (from external  $\text{SiMe}_4$ ) for the pendant-arm carbons are assigned as  $>\text{NCH}_2\text{CH}_2\text{OH}$  (57.38, 57.35 and 58.43) and  $>\text{NCH}_2\text{CH}_2\text{OH}$  (53.28, 54.89 and 59.05) and for the macrocyclic ring carbons (49.61 and 49.08, 50.30 and 48.94, and 52.49 and 49.98). (These assignments are based on that of the free  $\text{L}^1$  resonances at  $\delta$  57.71, 54.87 and 49.57 at 219.3 K to  $>\text{NCH}_2\text{CH}_2\text{OH}$ ,  $>\text{NCH}_2\text{CH}_2\text{OH}$  and the macrocyclic ring, respectively. Apart from some broadening near the solution freezing point, the resonance of the free  $\text{L}^1$  macrocyclic ring shows no tendency to resolve into a doublet.) For  $[\text{LiL}^1]^+$ ,  $[\text{NaL}^1]^+$  and  $[\text{KL}^1]^+$ , respectively, the difference in magnetic environments for  $>\text{NCH}_2\text{CH}_2\text{OH}$  and  $>\text{NCH}_2\text{CH}_2\text{OH}$ , reflected in  $\Delta\delta$ , changes in the sequence 4.10, 2.46 and  $-0.62$  ppm, and for the macrocyclic ring carbons in the sequence 0.53, 1.36 and 2.51 ppm. The change in the relative  $\delta$  of  $>\text{NCH}_2\text{CH}_2\text{OH}$  and  $>\text{NCH}_2\text{CH}_2\text{OH}$  for  $[\text{KL}^1]^+$  compared with those for  $[\text{LiL}^1]^+$  and  $[\text{NaL}^1]^+$  is deduced from the spectral coalescences of the resonances of  $\text{L}^1$  and  $[\text{ML}^1]^+$  during intermolecular exchange as discussed below.

As the temperature increases the two macrocyclic ring resonances of  $[\text{ML}^1]^+$  broaden and coalesce (Figs. 3 and 4) as methylene exchange between two different magnetic environments becomes faster, and complete lineshape analyses yield the rate parameters in Table 3. For  $[\text{LiL}^1]^+$  these parameters were derived from the following mean enantiomer lifetimes,  $\tau_c/\text{ms}$ , determined over temperature ranges where the exchange-induced resonance modifications were substantial and where the values in parentheses are the corresponding temperatures (K): 165 (204.7), 89.5 (209.9), 49.3 (215.1), 25.5 (220.3), 15.3 (225.5), 8.17 (230.8), 5.16 (236.0) and 2.88 (241.2). The corresponding data for  $[\text{NaL}^1]^+$  are 3.08 (230.8), 2.54 (236.0), 1.73 (241.2), 1.45 (246.4), 1.05 (251.6), 0.84 (256.9), 0.65 (262.1), 0.38 (272.5), 0.30 (277.8) and 0.26 (283.0), and for  $[\text{KL}^1]^+$  are 26.7 (241.2), 16.7 (246.4), 9.28 (251.6), 5.41 (256.9), 3.39 (262.1), 2.13 (267.3), 1.27 (272.5), 0.73 (277.8), 0.43 (283.0), 0.31 (288.2), 0.19 (293.4), 0.15 (297.0) and 0.10 (304.4).

The coalescence of the two macrocyclic ring resonances of  $[\text{LiL}^1]^+$  and  $[\text{NaL}^1]^+$  and the absence of change in the pendant-arm resonances (apart from a slight broadening attributable to solution viscosity increases at lower temperatures) is consistent with exchange between the two approximately square-antiprismatic enantiomers of each of the complexes (Fig. 5). A similar situation holds for  $[\text{KL}^1]^+$  except that the chemical shift difference between the two pendant-arm resonances decreases with increase in temperature such that they coincide at 304.4 K (Fig. 4). Enantiomerisation interchanges the magnetic environments of the macrocyclic ring carbons at sites *a* and *b* (although the two resonances arising

**Table 2** Parameters for exchange of Na<sup>+</sup> in [NaL<sup>n</sup>]<sup>+</sup>

Complex	Solvent	10 <sup>-5</sup> <i>k<sub>e</sub></i> (298.2 K)/ dm <sup>3</sup> mol <sup>-1</sup> s <sup>-1</sup>	<i>k<sub>d</sub></i> (298.2 K)/ s <sup>-1</sup>	Δ <i>H<sub>d</sub></i> <sup>‡</sup> / kJ mol <sup>-1</sup>	Δ <i>S<sub>d</sub></i> <sup>‡</sup> / J K <sup>-1</sup> mol <sup>-1</sup>
[NaL <sup>1</sup> ] <sup>+</sup> <sup>a</sup>	Acetonitrile <sup>a</sup>	3590	78.5 ± 1.0	49.2 ± 0.3	-43.7 ± 0.9
	Propylene carbonate <sup>a</sup>	8066	26.1 ± 0.6	57.7 ± 0.4	-24.0 ± 1.0
	Methanol <sup>b</sup>	70.8	209	68.3	28.4
	Dimethylformamide <sup>b</sup>	7.00	299	56.4	-8.4
[NaL <sup>3</sup> ] <sup>+</sup>	Methanol <sup>c</sup>	31	2.50		
[NaL <sup>4</sup> ] <sup>+</sup>	Methanol <sup>c</sup>	1700	0.0235		

<sup>a</sup> This work. Errors represent one standard deviation for the fit of the τ<sub>e</sub> data by equation (2). <sup>b</sup> Ref. 6. <sup>c</sup> Ref. 24.

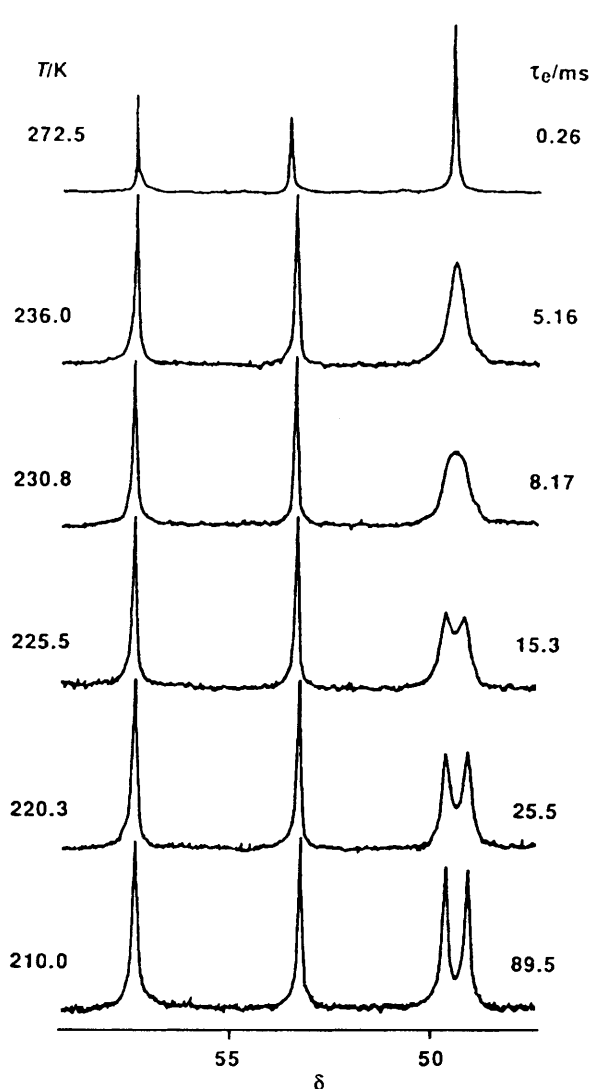


**Fig. 3** Typical exchange-modified 75.47 MHz <sup>13</sup>C NMR spectra of a 0.10 mol dm<sup>-3</sup> solution of [LiL<sup>1</sup>]ClO<sub>4</sub> in <sup>12</sup>C-enriched [<sup>2</sup>H<sub>4</sub>]methanol. Experimental temperatures and derived τ<sub>e</sub> values appear to the left and the right of the figure, respectively

from them cannot be separately assigned from the present data), whereas the pendant-arm carbons in sites *c* and *d* experience no change in magnetic environment. The approximately square-antiprismatic [ML<sup>1</sup>]<sup>+</sup> enantiomer structures are probably similar to those seen in the solid state for [KL<sup>1</sup>]<sup>+</sup>.<sup>9,11</sup> (The solid-state structures of [LiL<sup>1</sup>]<sup>+</sup> and [NaL<sup>1</sup>]<sup>+</sup> in which only three and one of the L<sup>1</sup> arms are bidentate, respectively, could not generate the observed <sup>13</sup>C NMR spectra if they persisted in solution.)

The rate parameters for intermolecular L<sup>1</sup> exchange on [ML<sup>1</sup>]<sup>+</sup>, as in equation (3), were determined from the coalescence of the <sup>13</sup>C resonances of >NCH<sub>2</sub>CH<sub>2</sub>OH and

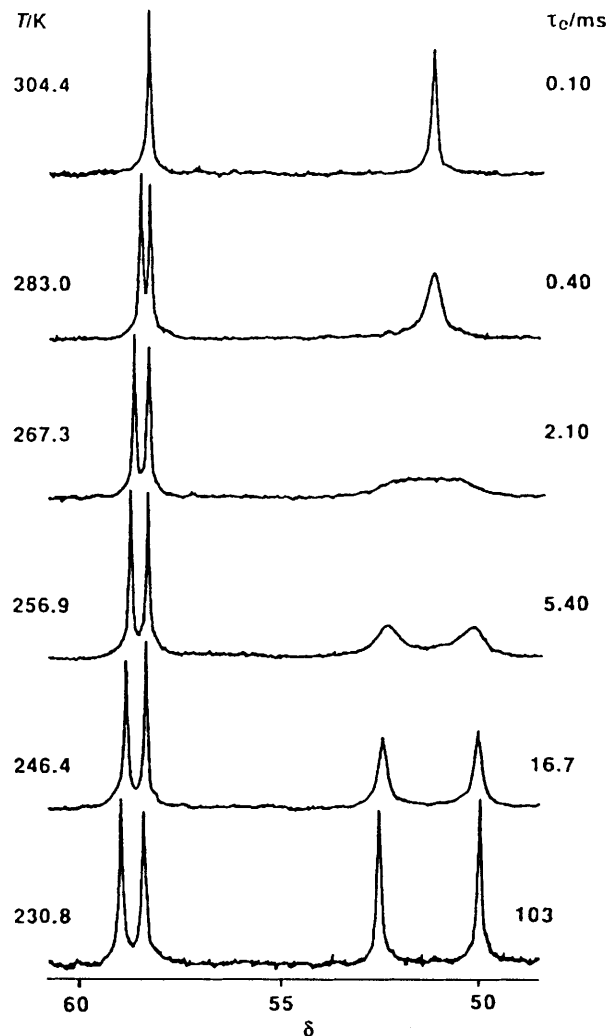
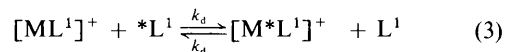


**Fig. 4** Typical exchange-modified 75.47 MHz <sup>13</sup>C NMR spectra of a 0.10 mol dm<sup>-3</sup> solution of [KL<sup>1</sup>][O<sub>3</sub>SCF<sub>3</sub>] in <sup>12</sup>C-enriched [<sup>2</sup>H<sub>4</sub>]methanol. Key as in Fig. 3



>NCH<sub>2</sub>CH<sub>2</sub>OH of free L<sup>1</sup> and [ML<sup>1</sup>]<sup>+</sup>, as illustrated for [KL<sup>1</sup>]<sup>+</sup> in Fig. 6, and are listed in Table 3. (The resonances arising from the macrocyclic rings of L<sup>1</sup> and [KL<sup>1</sup>]<sup>+</sup> coalesce because of the intermolecular exchange and the resulting enantiomerisation as discussed below.) The rate parameters shown in Table 3 were derived from the following mean [KL<sup>1</sup>]<sup>+</sup> lifetimes, τ<sub>e</sub>/ms, determined over temperature ranges where the exchange-induced resonance modifications were substantial and where the values in parentheses are the corresponding temperatures (K): 93.9 (223.6), 29.2 (234.1), 16.5 (239.3), 10.2 (244.5), 5.21 (249.7), 2.84 (254.9), 1.75 (260.1), 0.91 (265.3), 0.65 (270.6), 0.44 (275.8), 0.32 (281.0), 0.21 (286.2) and

**Table 3** Enantiomerisation and ligand-exchange parameters for  $[ML^1]^+$  in  $^{12}\text{C}$ -enriched  $[^2\text{H}_4]$ methanol determined by  $^{13}\text{C}$  NMR spectroscopy<sup>a</sup>

$M^+$	Process	$k/s^{-1}$ ( $T/K$ )	$k(298.2\text{ K})/$ $s^{-1}$	$\Delta H^\ddagger/$ $\text{kJ mol}^{-1}$	$\Delta S^\ddagger/$ $\text{J K}^{-1} \text{ mol}^{-1}$	$10^{-5} k_c(298.2\text{ K})^b/$ $\text{dm}^3 \text{ mol}^{-1} \text{ s}^{-1}$
$\text{Li}^+$	Enantiomerisation	$109 \pm 4$ (230.8)	$18\,300 \pm 3\,100$	$41.3 \pm 1.3$	$-24.8 \pm 5.9$	5.2
	$L^1$ exchange	$215 \pm 3$ (286.2) <sup>c</sup>	$424 \pm 7^e$	$37.7 \pm 0.5$	$-68.2 \pm 1.7$	
		$40 \pm 1$ (260.1) <sup>d</sup>				
$\text{Na}^+$ <sup>f</sup>	Enantiomerisation	$1237 \pm 17$ (256.9)	$7\,100 \pm 220$	$24.6 \pm 0.5$	$-88.6 \pm 1.8$	112.5
	$L^1$ exchange	$62 \pm 2$ (281.0) <sup>c</sup>	$332 \pm 8^e$	$65.6 \pm 0.8$	$23.3 \pm 3.0$	
		$105 \pm 3$ (286.2) <sup>d</sup>				
$\text{K}^+$	Enantiomerisation	$515 \pm 11$ (267.3)	$7\,010 \pm 200$	$53.7 \pm 0.6$	$8.8 \pm 2.3$	33.1
	$L^1$ exchange	$332 \pm 12$ (254.9) <sup>c</sup>	$12\,300 \pm 700^e$	$50.5 \pm 0.9$	$2.8 \pm 3.7$	
		$37 \pm 2$ (234.1) <sup>d</sup>				

<sup>a</sup> Errors represent one standard deviation for the fit of the  $\tau_c$  data by equation (2). <sup>b</sup> Complexation rate constant  $k_c (=k_dK)$ . <sup>c,d</sup> Decomplexation rate constants ( $k_d$ ) at  $>\text{NCH}_2\text{CH}_2\text{OH}$  and  $>\text{NCH}_2\text{CH}_2\text{OH}$  resonance-coalescence temperatures, respectively. <sup>e</sup> Decomplexation rate constants ( $k_d$ ) simultaneously determined from the  $>\text{NCH}_2\text{CHOH}$  and  $>\text{NCH}_2\text{CH}_2\text{OH}$  resonance coalescences. <sup>f</sup> Ref. 7.

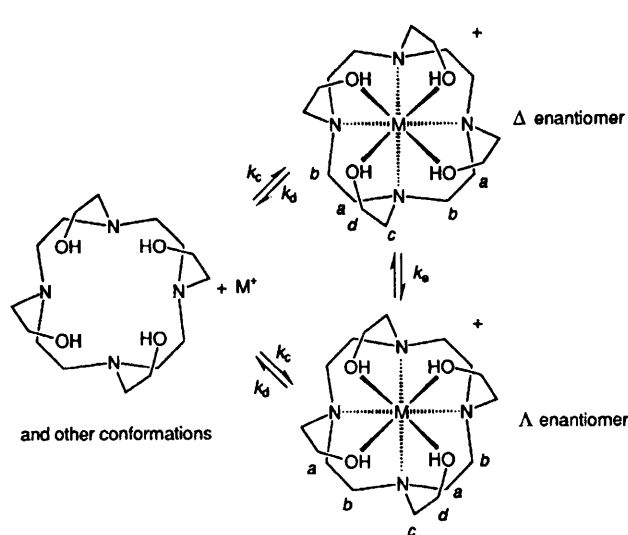


**Fig. 5** Intermolecular  $M^+$  exchange and intramolecular exchange between the  $\Delta$  and  $\Lambda$  square-antiprismatic enantiomers of  $[ML^1]^+$ . The  $\Delta$  and  $\Lambda$  enantiomers are designated as those in which a right- and left-hand chirality is observed, respectively, when the structure is viewed from the centre of the plane of the four oxygens looking towards  $M^+$  and the plane of the four nitrogens beyond it

0.10 (296.6). The analogous data for  $[\text{LiL}^1]^+$  are 130 (239.3), 53.5 (249.7), 37.3 (254.9), 21.7 (260.1), 18.1 (265.3), 12.2 (270.6), 8.91 (275.8), 6.68 (281.0), 5.25 (286.2), 3.44 (291.4), 2.54 (296.6), 1.65 (304.2), 1.28 (309.5), 0.98 (314.8) and 0.61 (325.4), and for  $[\text{NaL}^1]^+$  are 333 (245.9), 155 (260.1), 82.7 (265.3), 48.8 (270.6), 30.3 (275.8), 17.9 (281.0), 10.6 (286.2), 5.68 (291.4), 3.09 (296.6), 1.60 (304.2), 1.07 (309.5), 0.67 (314.8) and 0.31 (325.4).

The data for  $L^1$  exchange on  $[\text{LiL}^1]^+$  in Table 3 are similar to  $k_d(298.2\text{ K}) = 729\text{ s}^{-1}$ ,  $\Delta H_d^\ddagger = 38.0\text{ kJ mol}^{-1}$ ,  $\Delta S_d^\ddagger = -62.8\text{ J K}^{-1} \text{ mol}^{-1}$  and  $k_c(298.2\text{ K}) = 8.97 \times 10^5\text{ dm}^3 \text{ mol}^{-1} \text{ s}^{-1}$  obtained from  $^7\text{Li}$  NMR studies<sup>6</sup> and those for  $[\text{NaL}^1]^+$  are similar to those obtained from  $^{23}\text{Na}$  NMR studies (Table 2), and are consistent with the same process being monitored at two different NMR frequencies for each of these systems and the relationship  $\tau_c = 1/k_d$  holds for both  $M^+$  and  $L^1$  exchange on  $[ML^1]^+$ . For both  $[\text{LiL}^1]^+$  and  $[\text{NaL}^1]^+$  the rates of intermolecular exchange are substantially slower than those of enantiomerisation consistent with the latter process occurring through an intramolecular mechanism which may involve either a concerted twisting process or the detachment of one or more arms. In contrast, at 298.2 K the rate of  $L^1$  exchange on  $[\text{KL}^1]^+$  is twice that of enantiomerisation consistent with intermolecular ligand exchange producing enantiomerisation for every second exchange of  $L^1$  on average. The similarity of the activation parameters for the two processes is consistent

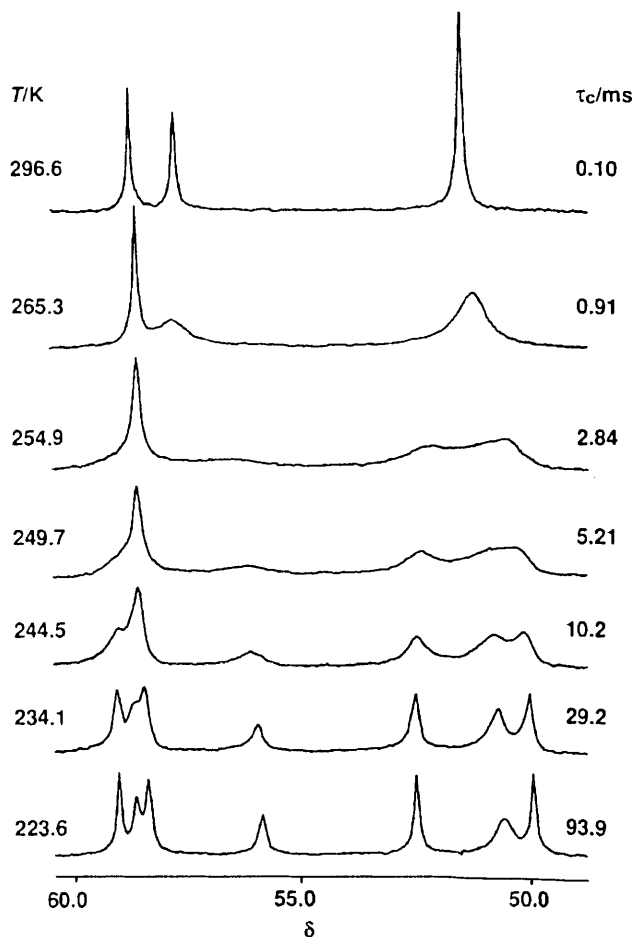


**Fig. 6** Typical exchange-modified 75.47 MHz  $^{13}\text{C}$  NMR spectra of a  $0.10\text{ mol dm}^{-3}$  solution of  $L^1$  and  $[\text{KL}^1][\text{O}_3\text{SCF}_3]$ , in  $^{12}\text{C}$ -enriched  $[^2\text{H}_4]$ methanol. Experimental temperatures and derived  $\tau_c$  values appear to the left and the right of the figure, respectively. At 223.6 K the resonances proceeding from left to right of the spectrum are assigned to  $>\text{NCH}_2\text{CH}_2\text{NOH}$  of  $[\text{KL}^1]^+$ ,  $>\text{NCH}_2\text{CH}_2\text{NOH}$  of  $L^1$ ,  $>\text{NCH}_2\text{CH}_2\text{NOH}$  of  $[\text{KL}^1]^+$ ,  $>\text{NCH}_2\text{CH}_2\text{NOH}$  of  $L^1$  and the macrocyclic ring carbons of  $[\text{KL}^1]^+$ ,  $L^1$  and  $[\text{KL}^1]^+$

with intermolecular ligand exchange being the dominant enantiomerisation mechanism for  $[\text{KL}^1]^+$ . This change in the relative importance of the inter- and intra-molecular processes for  $[ML^1]^+$  enantiomerisation arises from the greater lability of  $[\text{KL}^1]^+$  towards  $L^1$  exchange. The variations in the kinetic parameters for both enantiomerisation and  $L^1$  exchange do not show a clear trend, which is consistent with a variation with  $M^+$  of bonding and ligand strain contributing to transition-state enthalpies and entropies in different ways in the three  $[ML^1]^+$ .

## Acknowledgements

We thank the Australian Research Council and the University of Adelaide for supporting this research.

## References

- 1 L. F. Lindoy, *The Chemistry of Macrocyclic Ligand Complexes*, Cambridge University Press, Cambridge, 1989.
- 2 R. M. Izatt, K. Pawlak, J. S. Bradshaw and R. L. Bruening, *Chem. Rev.*, 1991, **91**, 1721.
- 3 G. W. Gokel, *Crown Ethers and Cryptands*, The Royal Society of Chemistry, Cambridge, 1991.
- 4 J.-M. Lehn and J. P. Sauvage, *J. Am. Chem. Soc.*, 1975, **97**, 6700.
- 5 J.-M. Lehn, *Pure Appl. Chem.*, 1979, **51**, 979.
- 6 M. L. Turonek, P. Clarke, G. S. Laurence, S. F. Lincoln, P.-A. Pittet, S. Politis and K. P. Wainwright, *Inorg. Chem.*, 1993, **32**, 2195.
- 7 R. Dhillon, A. K. W. Stephens, S. Whitbread, S. F. Lincoln and K. P. Wainwright, *J. Chem. Soc., Chem. Commun.*, 1995, 97.
- 8 R. D. Shannon, *Acta Crystallogr., Sect. A*, 1976, **32**, 751.
- 9 S. Buøen, J. Dale, P. Groth and J. Krane, *J. Chem. Soc., Chem. Commun.*, 1982, 1172.
- 10 P. Groth, *Acta Chem. Scand., Ser. A*, 1983, **37**, 71.
- 11 P. Groth, *Acta Chem. Scand., Ser. A*, 1983, **37**, 283.
- 12 S. Buøen, J. Dale and J. Krane, *Acta Chem. Scand., Ser. B*, 1984, **38**, 773.
- 13 J. E. Richman and T. J. Atkins, *J. Am. Chem. Soc.*, 1974, **96**, 2268.
- 14 D. D. Perrin, W. L. F. Aramaego and D. R. Perrin, *Purification of Laboratory Chemicals*, 2nd edn., Pergamon, Oxford, 1980.
- 15 S. F. Lincoln, *Prog. React. Kinet.*, 1977, **9**, 1.
- 16 B. G. Cox, H. Schneider and J. J. Stroka, *J. Am. Chem. Soc.*, 1978, **100**, 4746.
- 17 V. Gutmann, *Coordination Chemistry in Nonaqueous Solutions*, Springer, Wien, 1968.
- 18 W. J. Dewitte and A. I. Popov, *J. Solution Chem.*, 1976, **5**, 231.
- 19 R. G. Pearson, *J. Am. Chem. Soc.*, 1963, **85**, 3533.
- 20 R. G. Pearson, *Coord. Chem. Rev.*, 1990, **100**, 403.
- 21 F. A. Cotton and G. Wilkinson, *Advanced Inorganic Chemistry*, 3rd edn., Interscience, New York, 1980.
- 22 H.-J. Buschmann, *Inorg. Chim. Acta*, 1985, **102**, 95.
- 23 B. G. Cox, J. Garcia-Rosas and H. Schneider, *J. Am. Chem. Soc.*, 1981, **103**, 1384.
- 24 S. F. Lincoln, I. M. Brereton and T. M. Spotswood, *J. Chem. Soc., Faraday Trans. 1*, 1985, 1623.
- 25 B. G. Cox, J. Garcia-Rosas and H. Schneider, *J. Am. Chem. Soc.*, 1981, **103**, 1054.

Received 17th July 1995; Paper 5/04681E